minerals

MDPI

Article

Quantitative in Situ X-ray Diffraction Analysis of Early Hydration of Belite-Calcium Sulfoaluminate Cement at Various Defined Temperatures

Maruša Borštnar [1,2,*], Christian L. Lengauer [3] and Sabina Dolenec [1]

[1] Slovenian National Building and Civil Engineering Institute, Dimičeva ulica 12, 1000 Ljubljana, Slovenia; sabina.dolenec@zag.si
[2] Jožef Stefan International Postgraduate School, Jamova cesta 39, 1000 Ljubljana, Slovenia
[3] Department of Mineralogy and Crystallography, University of Vienna, UZA 2, Althanstraße 14, 1090 Vienna, Austria; christian.lengauer@univie.ac.at
* Correspondence: marusa.borstnar@zag.si

Abstract: The influence of temperature on the early hydration of belite-calcium sulfoaluminate cements with two different calcium sulfate to calcium sulfoaluminate molar ratios was investigated. The phase composition and phase assemblage development of cements prepared using molar ratios of 1 and 2.5 were studied at 25, 40 and 60 °C by in situ X-ray powder diffraction. The Rietveld refinement method was used for quantification. The degree of hydration after 24 h was highest at ambient temperatures, but early hydration was significantly accelerated at elevated temperatures. These differences were more noticeable when we increased the temperature from 25 °C to 40 °C, than it was increased from 40 °C to 60 °C. The amount of calcium sulfate added controls the amount of the precipitated ettringite, namely, the amount of ettringite increased in the cement with a higher molar ratio. The results showed that temperature also affects full width at half maximum of ettringite peaks, which indicates a decrease in crystallite size of ettringite at elevated temperatures due to faster precipitation of ettringite. When using a calcium sulfate to calcium sulfoaluminate molar ratio of 1, higher d-values of ettringite peaks were observed at elevated temperatures, suggesting that more ions were released from the cement clinker at elevated temperatures, allowing a higher ion uptake in the ettringite structure. At a molar ratio of 2.5, less clinker is available in the cement, therefore these differences were not observed.

Keywords: in situ X-ray diffraction; hydration; temperature; cement; Rietveld analysis

Citation: Borštnar, M.; Lengauer, C.L.; Dolenec, S. Quantitative in Situ X-ray Diffraction Analysis of Early Hydration of Belite-Calcium Sulfoaluminate Cement at Various Defined Temperatures. *Minerals* **2021**, *11*, 297. https://doi.org/10.3390/min11030297

Academic Editor: Thomas N. Kerestedjian

Received: 4 February 2021
Accepted: 9 March 2021
Published: 11 March 2021

1. Introduction

The trend towards sustainability and lowering the carbon footprint has led to the development and production of new mineral binders. Within this context, iron-rich belite-calcium sulfoaluminate, also known as sulfobelite cements [1–3] or belite-ye'elimite-ferrite [4–6] cements, represent a low carbon and low energy alternative to ordinary Portland cement. Up to 35% less CO_2 is released during the production of belite-calcium sulfoaluminate cements compared to ordinary Portland cement. Furthermore, belite-calcium sulfoaluminate clinkers demand lower clinkering temperatures (1250–1350 °C in comparison to around 1450 °C) and are easier to grind [7–9]. One of the advances is also the replacement of a part of raw materials with industrial by-products and waste [1,5,10–12].

Belite-calcium sulfoaluminate cement clinkers are usually described to contain around 40–75 wt. % belite, 15–35 wt. % calcium sulfoaluminate, and 5–25 wt. % ferrite [7,13]. They are typically prepared by adding varying amounts of calcium sulfate in order to achieve the optimal compressive strength, setting time and volume stability [14–16]. The hydration of these cements depends on several factors, including the composition of the cement clinker, polymorphism of the clinker phases present, the presence of minor phases,

and the water-to-binder ratio, amongst others [4,9,17–21]. One of the major factors affecting hydration is temperature, which influences hydration kinetics, phase assemblage, and the rheological and mechanical properties of cement [18,22–24]. Different weather conditions, and the amount of heat released during the hydration process, may therefore have a significant impact on cementitious materials [25,26].

One of the main and important phases of belite-calcium sulfoaluminate cements, which reacts at an early age, is calcium sulfoaluminate ($C_4A_3\bar{S}$; hereafter cement notation was used throughout the paper: C = CaO, S = SiO_2, A = Al_2O_3, F = Fe_2O_3, $\bar{S}$ = SO_3, N = N_2O, K = K_2O, T = TiO_2, H = H_2O), the synthetic analogue of the sodalite-type mineral ye'elimite, $Ca_4Al_6(SO_4)O_{12}$. Calcium sulfoaluminate causes rapid strength development and controls the evolution of early cement performance, setting, and hardening [5,18,27–29]. The hydration of calcium sulfoaluminate, and the formation of hydration products, strongly depend on the type and amount of calcium sulfate (anhydrite $C\bar{S}$, gypsum $C\bar{S}H_2$ or bassanite $C\bar{S}H_{0.5}$) added [14,18,27]. When the molar ratio of calcium sulfate to calcium sulfoaluminate is below 2 (M-value < 2), and until the added calcium sulfate is depleted, the main crystalline hydration product formed is ettringite-type $C_6A\bar{S}_3H_{32}$, which precipitates together with amorphous aluminum hydroxide (AH_3) according to the reaction shown in Equation (1) [14,20,27,30]:

$$C_4A_3\bar{S} + 2C\bar{S}H_x + (38 - 2x)H \rightarrow C_6A\bar{S}_3H_{32} + 2\,AH_3\ (x = 0, 0.5, 2), \quad (1)$$

In case the molar ratio of calcium sulfate to calcium sulfoaluminate exceeds the value of 2 (M-value > 2), besides ettringite, surplus calcium sulfate is also present [14,15].

In the absence of calcium sulfate, or when the calcium sulfate source is depleted, the main hydration products formed are monosulfate ($C_4A\bar{S}H_{12}$) and aluminum hydroxide [14,27,28,30], according to Equation (2).

$$C_4A_3\bar{S} + 18H \rightarrow C_6A\bar{S}H_{12} + 2AH_3, \quad (2)$$

The M-value is also used to designate the type of calcium sulfoaluminate cement, where M < 1.5 classifies cements with rapid hardening and high strength, an M value between 1.5 and 2.5 defines expansive cements, and M > 2.5 refers to self-stressing cements [15,31].

At an advanced hydration age, belite (C_2S), the synthetic analogue of another important clinker phase, the mineral larnite (Ca_2SiO_4), starts to react. This primarily contributes to the late compressive strength of the cement [16,18]. Belite, together with aluminum hydroxide and the addition of water, may yield either strätlingite-type C_2ASH_8 [30], according to Equation (3), or amorphous calcium silicate hydrate (C–S–H) and portlandite-type CH after the depletion of aluminum hydroxide [30], according to reaction Equation (4).

$$C_2S + AH_3 + 5H \rightarrow C_2ASH_8, \quad (3)$$

$$C_2S + nH \rightarrow C\text{-}S\text{-}H + mCH, \quad (4)$$

Furthermore, katoite-type C_3ASH_4 can precipitate in the reaction of strätlingite with portlandite [30], according to Equation (5):

$$C_2ASH_8 + CH \rightarrow C_3ASH_4, \quad (5)$$

Early hydration is an important period, which determines the fresh properties of concrete and also its final mechanical properties and durability [18,32]. Moreover, most of the hydration heat of cement, as determined by isothermal calorimetry, evolves within the first 24 h of hydration [1]. The most prominent method to study phase composition and the development of phase assemblage in the hardening paste is powder X-ray diffraction (PXRD) [29,32,33]. Through in situ analysis of PXRD patterns by Rietveld refinement [34], the quantitative phase composition of the cement samples during early hydration reactions could be determined [12,33].

The early hydration reactions of belite-calcium sulfoaluminate cement pastes, with different amounts and sources of added calcium sulfate, have already been studied by in situ PXRD, but only at ambient temperatures [1,12]. The early reactions in these cement pastes at ambient temperatures were also investigated by Bullerjahn et al. [5], who focused their study on the effect of boron during early hydration. Studies of the early age hydration of calcium sulfoaluminate at ambient temperature were evaluated by Zajac et al. [28] and Jansen et al. [27] At elevated temperatures (55 and 85 °C), the hydration in the first 24 h was studied only on calcium sulfoaluminate cements, however, just a qualitative phase analysis was performed. Despite the fact that the literature provides some studies of early hydration reactions, a detailed study of early age hydration phases of belite-calcium sulfoaluminate cements at different temperatures has not been presented to date.

The aim of the present study was to characterize the influence of different temperatures on the phase composition of belite-calcium sulfoaluminate cement pastes during the first 24 h of hydration, while comparing pastes of different calcium sulfate to calcium sulfoaluminate molar ratios. To determine the hydration phase assemblage and investigate the influence of the amount of calcium sulfate source on the formation of hydration products, in situ PXRD measurements and quantitative analysis using the Rietveld method were performed on cements with M-values of 1 and 2.5 at 25, 40 and 60 °C.

2. Materials and Methods

The targeted phase composition of the cement clinker used for the study was 65.0 wt. % belite (C_2S), 20.0 wt. % calcium sulfoaluminate ($C_4A_3\bar{S}$) and 10.0 wt. % ferrite (C_4AF) [35]. In order to obtain the targeted phase composition, the raw materials (calculated to Total = 95 wt. %) were proportioned using an adapted Bogue method [22]. The Bogue calculation is only used to determine the phase composition of the main phases, while the minor phases are neglected [36]. The clinker was synthesized from the following raw materials: limestone (57.9 wt. %), flysch (sedimentary rock sequence consisting of layers of calcareous breccia, calcareous sandstones and marls; 23.6 wt. %), bottom ash from a coal thermal power plant (9.0 wt. %), calcined bauxite (5.3 wt. %), white titanogypsum (4.0 wt. %) and mill scale (0.2 wt. %). The chemical composition of the raw meal used has been described by Dolenec et al. [37], while the chemical composition of the raw materials and the proportions were presented in the study by Borštnar et al. [24] The phase composition of the clinker, obtained by Rietveld refinement, is given in Table 1, where the amount of calcium sulfoaluminate is the sum of the orthorhombic and cubic polymorph, and the amount of belite is the sum of β-belite and γ-belite.

Table 1. Calculated targeted and observed phase composition of the synthesized cement clinker as obtained by Rietveld refinement in wt. %.

	Σ Belite	Σ Calcium Sulfoaluminate	Ferrite	Mayenite	Periclase	Gehlenite	Arcanite	Aphthitalite
Targeted phase composition (wt. %)	65.0	20.0	10.0	-	-	-	-	-
Observed phase composition (wt. %)	65.7	17.7	11.6	2.5	1.1	0.4	0.4	0.6

Raw materials were first ground and sieved through a 200 μm mesh and then homogenized. Each 200 g batch of proportioned raw materials was dispersed in 200 mL of isopropanol, mixed for 3 h in a ball mill (Capco Ball Mill 9VS, Capco Test Equipment, Ipswich, IP1 5AP, UK), and then dried in a 40 °C oven for 24 h; 15 g of the raw meal was subsequently pressed into pellets 30 mm wide and 13 mm high using an HPM 25/5 press at 10.6 kN. The pellets were placed in a Protherm PLF 160/9 (Protherm Furnaces, Ankara, Turkey) furnace and fired to 1250 °C at a heating rate of 10 °C/min. Following this,

they were held at the final temperature for 60 min and then cooled in the closed furnace for 20 h. The entire process was performed under oxidizing conditions.

Before blending the synthesized clinker with white titanogypsum (ground < 0.125 mm), the clinker was first hand-crushed using an agate mortar and ground to less than 0.125 mm using a vibratory disc mill (Siebtechnik TS. 250, Siebtechnik GmbH, Mülheim an der Ruhr, Germany). Two cements were prepared with different proportions of white titanogypsum, based on the M-value, which designates the molar ratio of calcium sulfate ($CaSO_4$) to calcium sulfoaluminate [14]. The cements were prepared by blending a ground cement clinker with 5.6 and 12.9 wt. % titanogypsum, which is equivalent to M = 1 and 2.5, respectively. These M-values were chosen to compare the influence of the amount of calcium sulfate on the formation of hydration products. At M = 1, the reactions defined in Equation (1) or (2) occur, whereas at M = 2.5 only the Equation (1) reaction takes place and surplus gypsum remains present in the system [14]. Next, 200 g of cement was ground for 5 h using the Capco ball mill. The Blaine specific surface area of the cements, determined according to standard test method EN 196-6 [38], was 5200 cm^2/g and 5990 cm^2/g for M = 1 and M = 2.5, respectively. The particle size distributions of the two cements, which are shown in Figure 1, were determined using a laser particle analyzer (Sync Microtrac MRB, dry operation, Microtrac MRB, Haan, Germany). The phase compositions of the unhydrated cements, as determined by the Rietveld method, are listed in Table 2.

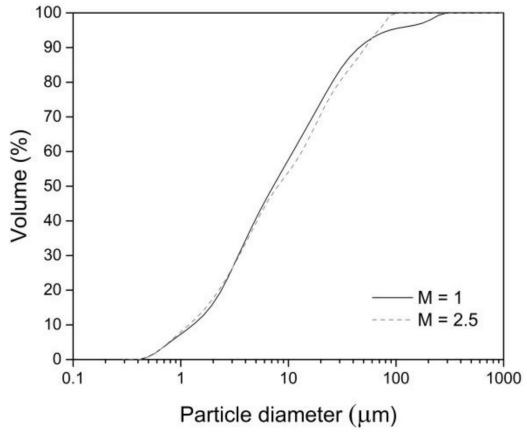

Figure 1. Particle size distributions of prepared cement mixtures with two molar ratios (M).

Table 2. Phase composition of unhydrated cements with M = 1 and M = 2.5 in wt. % determined with Rietveld method.

	M = 1	M = 2.5
Calcium sulfoaluminate-orthorhombic	8.0	6.8
Calcium sulfoaluminate-cubic	10.7	10.3
Σ Calcium sulfoaluminate	18.7	17.1
Belite-beta	58.0	53.4
Belite-gamma	5.1	5.3
Σ Belite	63.1	58.7
Ferrite	9.1	8.5
Periclase	0.9	0.8
Mayenite	1.4	1.1
Gehlenite	0.4	0.6
Arcanite	0.1	0.1
Aphthitalite	0.5	0.4
Gypsum	5.7	12.8

In situ PXRD measurements were performed to study the phase formation of the cement pastes during the early age hydration process within the first 24 h.

The prepared cements were mixed with deionized water in a water to cement ratio of 0.6 and manually stirred for 1 min. The mixture was then immediately cast in the sample holder (14 mm diameter, 1 mm depth). Measurements were performed at 25, 40 and 60 °C, at a relative humidity of 95 ± 2 %, using an Anton Paar XRK900 (Anton Paar GmbH, Graz, Austria) reactor chamber without internal Be-shielding and an automated z-alignment stage. The temperature-specific maximum relative humidity was established by continuous flow (20 mL/min) of water saturated gas (N_2) combined by heating the XRK900 chamber together with an external heating/cooling device for avoiding vapor condensation.

PXRD patterns of the cement pastes were obtained using a Bruker D8-Advance theta-theta goniometer (Bruker, Massachusetts, ZDA), equipped with a LynxEye position-sensitive detector. CuKa radiation was used at 40 kV and 40 mA, using a primary Ni-filter, an automatic divergence slit (l = 12 mm), and 2.3° primary and secondary soller slits. Measurements were performed from 5 to 75 °2θ, at increments of 0.02 °2θ/min, with an overall counting time of 20 min per scan. Under these conditions, 69 X-ray diffraction patterns per sample were collected in repetition mode during the first 24 h of hydration.

The obtained PXRD patterns of cement pastes at different temperatures were analyzed using X'Pert High Score Plus diffraction software v. 4.9 from PANalytical (Malvern Panalytical, Malvern, Worcestershire, United Kingdom), using PAN ICSD v. 3.4 powder diffraction data database. For qualitative phase analyses the entries of ICDD PDF 4+ 2020 RDB powder diffraction files were used. The initial crystal structural models used for the Rietveld refinements of the cementitious phases [39] were taken from Cuesta et al. [40,41] for orthorhombic and cubic calcium sulfoaluminate, for the other identified phases entries of the ICSD (Inorganic Crystal Structure Data) were applied, as listed in Table 3. First, the overall zero error and phase scale factors were refined and the background was fitted to a cosine Chebyshev function of 10 polynomial terms. Furthermore, the cell parameters and phase-specific Lorentzian functions (CS_L parameters) allowing for peak shape broadening were included in the refinement. For the determination of X-ray amorphous content, corundum (Al_2O_3, NIST SRM 676a) was used as an external standard.

Table 3. Phase designations and ICSD entries used for the Rietveld refinement.

Phase	Cement Notation	ICSD	References
Calcium sulfoaluminate-orthorhombic	$C_4A_3\bar{S}$	237892	[40]
Calcium sulfoaluminate-cubic	$C_4A_3\bar{S}$	194482	[41]
Belite-beta	β-C_2S	81096	[42]
Belite-gamma	γ-C_2S	81095	[42]
Ferrite	C_4AF	98836	[43]
Gypsum	$C\bar{S}H_2$	409581	[44]
Periclase	M	9863	[45]
Mayenite	$C_{12}A_7$	261586	[46]
Gehlenite	C_2AS	158171	[47]
Arcanite	$K_2\bar{S}$	79777	[48]
Aphthitalite	$K_3N\bar{S}_2$	26818	[49]
Ettringite	$C_6\bar{S}_3H_{32}$	155395	[50]

In order to determine the degree of hydration of clinker phases, the obtained phase composition of cement clinker was normalized to paste content, taking into account the amount of water added at time 0.0 h of hydration (w/c = 0.6). The degree of hydration of selected phases (calcium sulfoaluminate and gypsum) was calculated by comparing the amount of individual anhydrous phase remaining in the cement paste to the amount of the normalized anhydrous phase in cement. To this end, also all the graphs are showing direct results of Rietveld refinement. Moreover, on the graphs β-C_2S and γ-C_2S is given as Σ belite and calcium sulfoaluminate-orthorhombic and -cubic as Σ calcium sulfoaluminate.

In order to assess differences in the composition of ettringite, and the influence of temperature on its composition and structure, d-values and full widths at half maximum

were studied. Ettringite was selected because it is the main hydrated phase in the early hydration of belite calcium sulfoaluminate cements. The strongest lines of powder diffraction pattern of ettringite with reference pattern 00-041-1451 [29,50] are at d-values of 9.720 Å and 5.610 Å, corresponding to Miller indices (hkl) of 100 and 110, respectively. The d-value, or interplanar spacing between atoms in the crystal, and full widths at half maximum (FHWM) of the (100) and (110) peaks of ettringite were collected and plotted at 20 min and every 100 min from the start of the hydration up to 24 h.

3. Results

3.1. Cement Hydration at 25 °C

Results of in situ X-ray diffraction analysis of the cement pastes at 25 °C with a molar ratio of calcium sulfate to calcium sulfoaluminate 1 and 2.5 are shown in Figure 2. Figure 3 plots the degrees of hydration for calcium sulfoaluminate and gypsum, i.e., the main constituents reacting during the first 24 h, as well as the increasing ettringite content as their main hydration product. Figure 4 shows the evolution of the X-ray diffraction patterns at selected hydration times of the two investigated mixtures at 25, 40 and 60 °C.

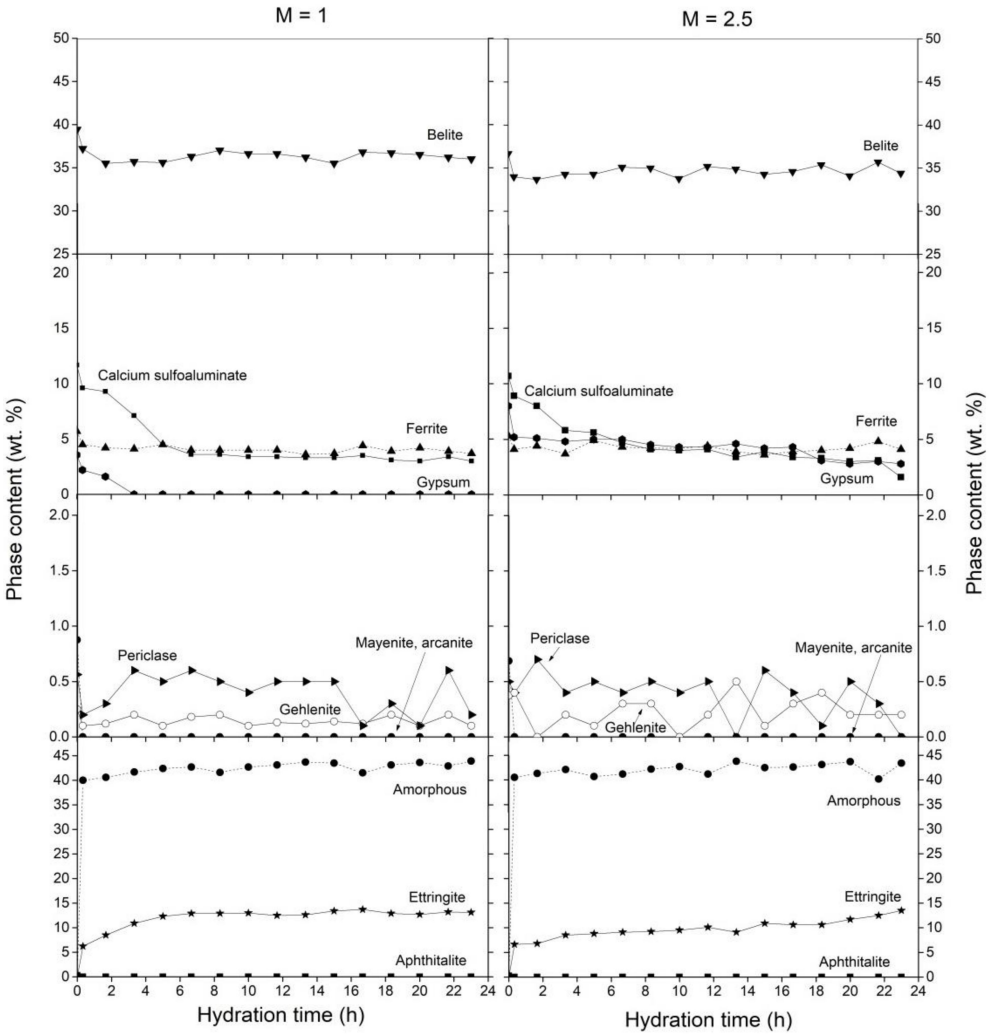

Figure 2. Phase content in the cement pastes with M = 1 and M = 2.5 cured at 25 °C during the first 24 h of hydration.

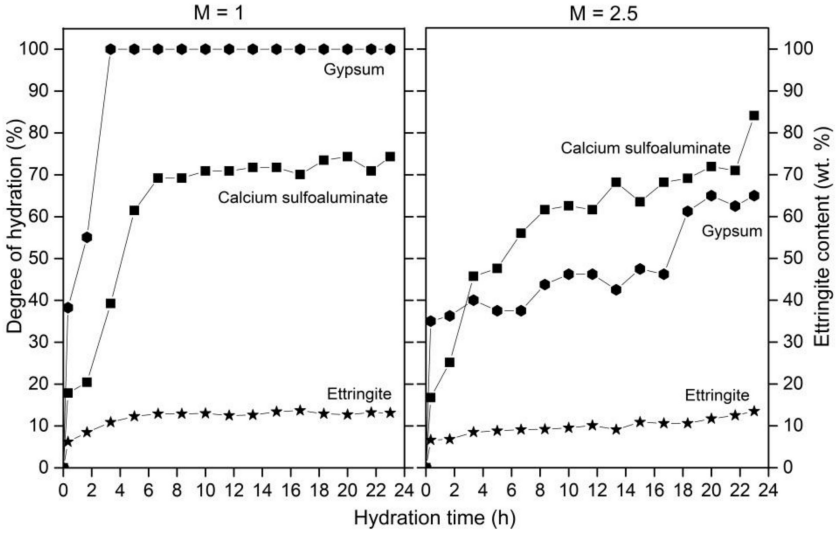

Figure 3. Degree of hydration of calcium sulfoaluminate and gypsum with ettringite content during the first 24 h of hydration of the M = 1 and M = 2.5 samples at 25 °C.

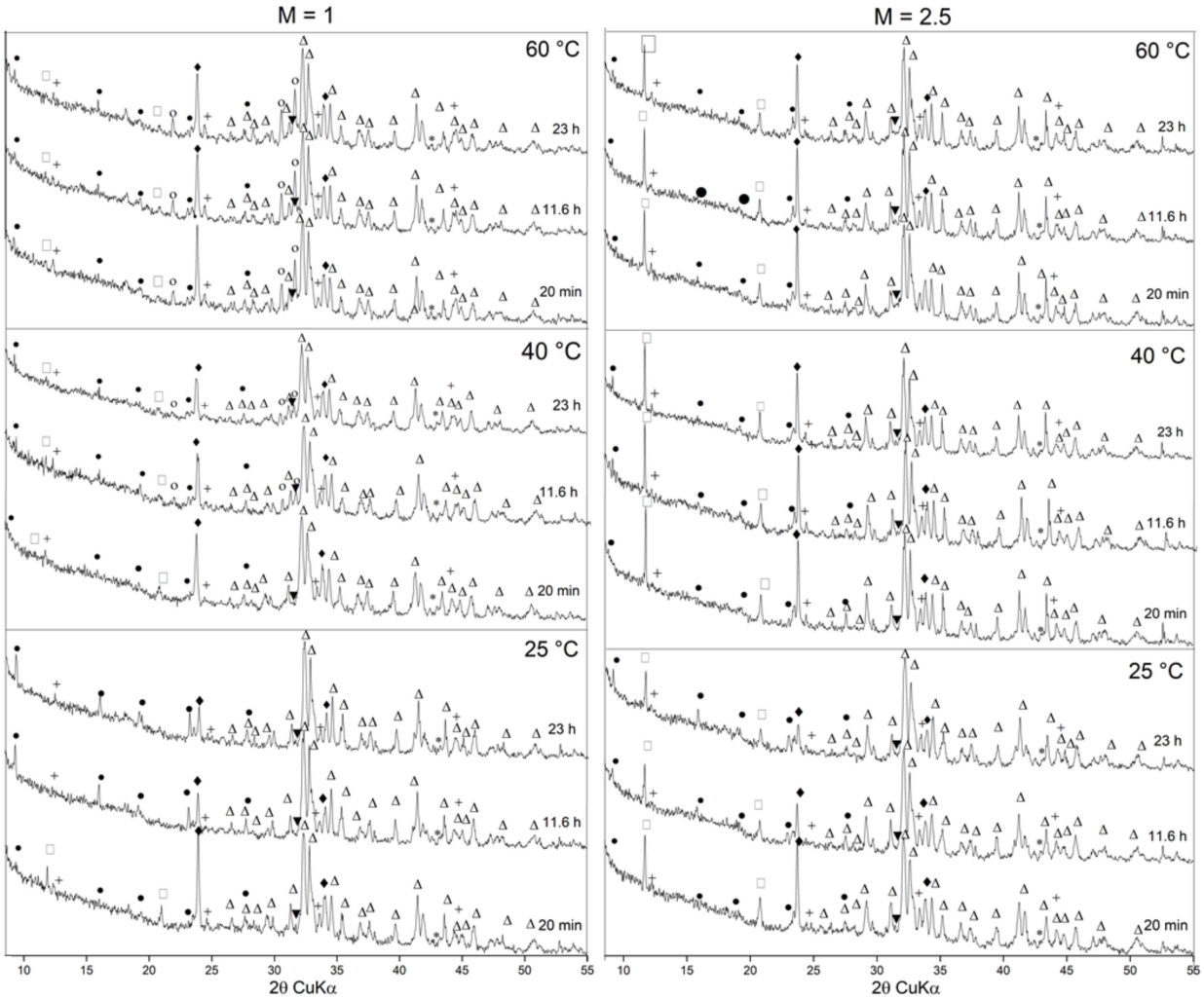

Figure 4. In situ X-ray powder diffraction patterns of the M = 1 and M = 2.5 samples at 25, 40 and 60 °C after 20 min, 11.6 and 23 h in a selected 2θ CuKα range. Δ = belite, ♦ = calcium sulfoaluminate, + = ferrite, □ = gypsum, ∗ = periclase, ▼ = gehlenite, ○ = aphthitalite, ● = ettringite.

The clinker phases identified in the cement paste with a molar ratio of 1 (M = 1) were belite, calcium sulfoaluminate, ferrite, gypsum, gehlenite, and periclase. The only provable crystalline hydrate in the cement pastes was ettringite. In addition, amorphous content was present. As seen from Figure 2, the early age hydration started immediately after adding the defined amount of water to the unhydrated cement. Within the first 5 h of hydration, therefore, calcium sulfoaluminate and gypsum were proportionally dissolved with a high degree of hydration (Figure 3). Within the first 5 h the amount of calcium sulfoaluminate decreased rapidly from 11.7 wt. % to 4.6 wt. %, indicating that 61.5 % of the calcium sulfoaluminate reacted in 5 h. After that, it decreased only slightly, to 3.0 wt. %, and reached its final degree of hydration at 74.3% (Figure 3), which indicates the amount of calcium sulfoaluminate which reacted in the first 24 h of hydration. The gypsum was completely depleted after 3 h. When the gypsum was consumed, the rate of dissolution of calcium sulfoaluminate slowed, remaining at almost the same level, as did the formation rate of ettringite. Simultaneously, the ettringite content increased during the first 5 h to 12.3 wt. %, while later on it increased slightly, to 13.1 wt. %. With ongoing hydration between 5 and 24 h, both the formation of ettringite and dissolution of calcium sulfoaluminate were much reduced, with only small changes in their amounts being observed. The amount of belite and ferrite did not significantly change within the first 24 h of the hydration process. Additionally, the minor clinker phase gehlenite was consumed after 20 min of hydration. The periclase content stayed almost constant throughout the hydration. Mayenite, arcanite and aphthitalite, which were all present in the unhydrated cement, were not detected. Amorphous content increased with the hydration time from 40.0 wt. % to 43.8 wt. %.

For the cement paste with a molar ratio of 2.5 (M = 2.5) the detected phases were belite, calcium sulfoaluminate, ferrite, gypsum, gehlenite, periclase and ettringite, in addition to amorphous content. At 25 °C, gypsum was measurable during 24 h of hydration. The results indicate a steady dissolution of calcium sulfoaluminate and gypsum, accompanied by the precipitation of ettringite as the major crystalline product. Over the first 3.3 h of the hydration, calcium sulfoaluminate rapidly diminished, from 10.7 wt. % to 5.7 wt. %. This was followed by a slow but continuous decline, until it reached a final value of 1.6 wt. % after 24 h, corresponding to the degree of hydration of calcium sulfoaluminate of 84.1 % (Figure 3). Accordingly, most of the gypsum reacted in the first 3.3 h of hydration from 8 wt. % to 4.7 wt. % and then only slowly decreased to 2.8 wt. % at 24 h. The degree of hydration of gypsum at 24 h was 65.0 %. The ettringite content constantly increased during hydration, increasing significantly to 8.6 wt. % in the first 3.3 h, then steadily increasing up to 13.5 wt. % at 24 h of hydration. Belite was observed in approximately the same amounts throughout the hydration, and the amounts of ferrite, periclase and gehlenite also did not significantly change in the first 24 h of hydration. Mayenite, arcanite and aphthitalite peaks, which were present in the unhydrated cement, were not observed. Furthermore, the amorphous content increased from 40.5 wt. % to 43.3 wt. % during hydration.

3.2. Cement Hydration at 40 °C

Results of in situ X-ray diffraction analysis of the cement pastes with molar ratios of 1 and 2.5 at 40 °C are shown in Figures 5 and 6. The evolution of the X-ray diffraction patterns at selected hydration times is given in Figure 4.

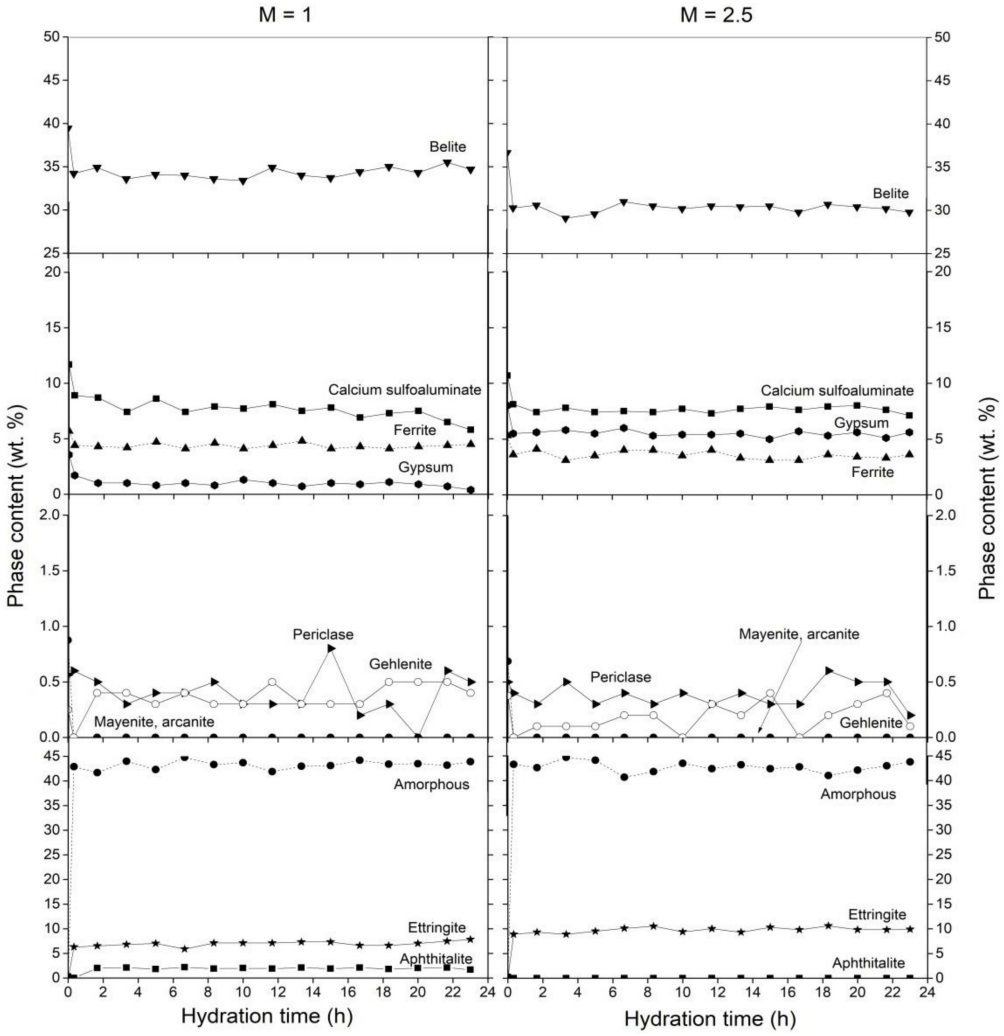

Figure 5. Phase content in the cement pastes with M = 1 and M = 2.5 cured at 40 °C during the first 24 h of hydration.

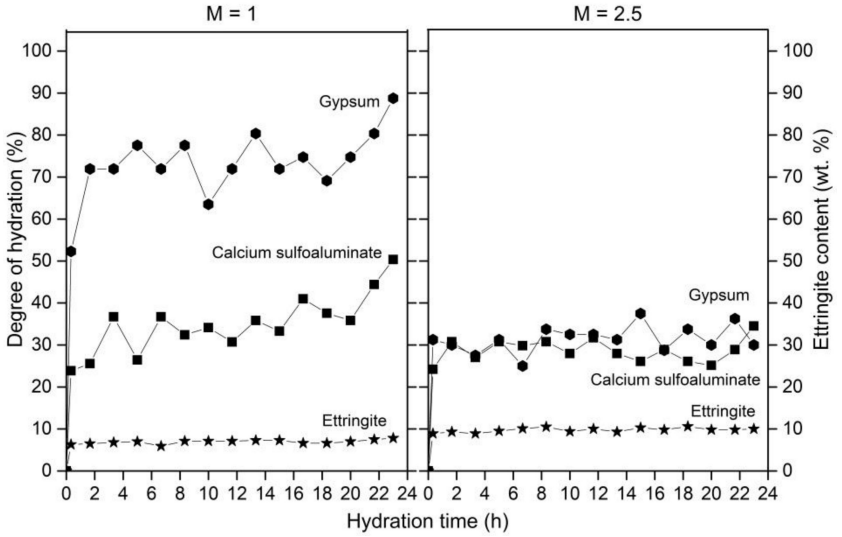

Figure 6. Degree of hydration of calcium sulfoaluminate and gypsum with ettringite content during the first 24 h hydration of the M = 1 and M = 2.5 samples at 40 °C.

At a molar ratio of 1, the following phases were identified: belite, calcium sulfoaluminate, ferrite, gypsum, aphthitalite, gehlenite, periclase, and ettringite, as the only

hydrated phase. In addition, amorphous content was present. After mixing with water the amount of calcium sulfoaluminate and gypsum declined sharply within the first 1.6 h, i.e., from 11.7 wt. % to 8.7 wt. % and from 3.6 wt. % to 1 wt. %, respectively. Accordingly, 36.7% of calcium sulfoaluminate and 71.9% of gypsum reacted during the first 1.6 h of hydration (Figure 6). Between 1.6 and 24 h, their amount declined slower, with gypsum remaining present in the amount of 0.4 wt. % after 24 h of hydration. After 24 h, the degree of hydration of calcium sulfoaluminate was 50.4% (5.8 wt. %). The results show that the main and only hydrate phase formed was ettringite, which increased to 6.5 wt. % within the first 1.6 h and reached a final value of 7.8 wt. % after 24 h of hydration. The contents of belite and ferrite exhibited no change over 24 h, which also held for the periclase and gehlenite content. Mayenite, arcanite and aphthitalite were clearly depleted in the first 20 min of hydration, while aphtitalite again appeared at 1.6 h with an amount of 1.6 wt. %, which then remained constant up to 24 h of hydration. Amorphous content was almost constant during hydration, with values between 42.0 and 43.0 wt. %.

Phase composition analysis of the mixture with a molar ratio of 2.5 (M = 2.5) at 40 °C showed that the phases present were belite, calcium sulfoaluminate, ferrite, gypsum, gehlenite and periclase. The only hydrate identified in the cement pastes was ettringite. Amorphous content was also present. The amounts of calcium sulfoaluminate and gypsum diminished in the first 20 min of hydration, in concert with the formation of ettringite. 2.5 wt. % of gypsum was consumed in the first 20 min, with calcium sulfoaluminate decreasing from 10.7 wt. % to 8.1 wt. %, but subsequently their amounts decreased slower. After 24 h the degree of hydration of calcium sulfoaluminate and gypsum was approximately 34.5% and 30.0%, respectively (Figure 6). Ettringite precipitated to the amount of 8.9 wt. % within the first 20 min of hydration, after which time it increased only slightly to 9.9 wt. %. The results showed no change in the amount of belite and ferrite. The quantities of periclase and gehlenite did not change significantly after 20 min of hydration. No mayenite, arcanite, and aphthitalite were detected. The amorphous content did not significantly change and it was around 43 wt. %.

3.3. Cement Hydration at 60 °C

Results of in situ X-ray diffraction analysis of the cement pastes at 60 °C with molar ratios of 1 and 2.5 are shown in Figures 7 and 8. The evolution of the X-ray diffraction patterns at selected hydration times is given in Figure 4.

The phases observed in the cement paste with a molar ratio calcium sulfate to calcium sulfoaluminate of 1 included belite, calcium sulfoaluminate, ferrite, gypsum, aphthitalite, gehlenite, and periclase as clinker phases, ettringite as a hydrated phase and amorphous content (Figure 7). The results show that hydration started directly after mixing the cement with water, by exhibiting a high degree of hydration of calcium sulfoaluminate and gypsum within the first 20 min. This caused the formation of ettringite, the only hydrate phase detected (Figure 8). After 20 min the amount of calcium sulfoaluminate decreased slightly, from 11.7 wt. % to 8.5 wt. %, when it converged to an almost constant value with a slow decrease with time. The results show that 27.3 wt. % of the calcium sulfoaluminate reacted in 20 min. Furthermore, at 60 °C all of the gypsum was dissolved to 1.3 wt. % within 20 min of the start of the reaction and reached a final degree of reaction after 23 h at 77.5 %. At the same time, ettringite rapidly increased to 5.6 wt. %, and then continuously increased to a maximum of 7.1 wt. % after 24 h. The belite and ferrite content did not significantly change at an early age. Periclase and gehlenite content remained almost constant throughout the hydration. Mayenite and arcanite were not detected after the hydration proceeded. Aphthitalite content increased from 0.5 wt. % to 4.6 wt. % in the first 20 min and stayed constant up to 24 h. Around 42 wt. % amorphous content was present during the hydration.

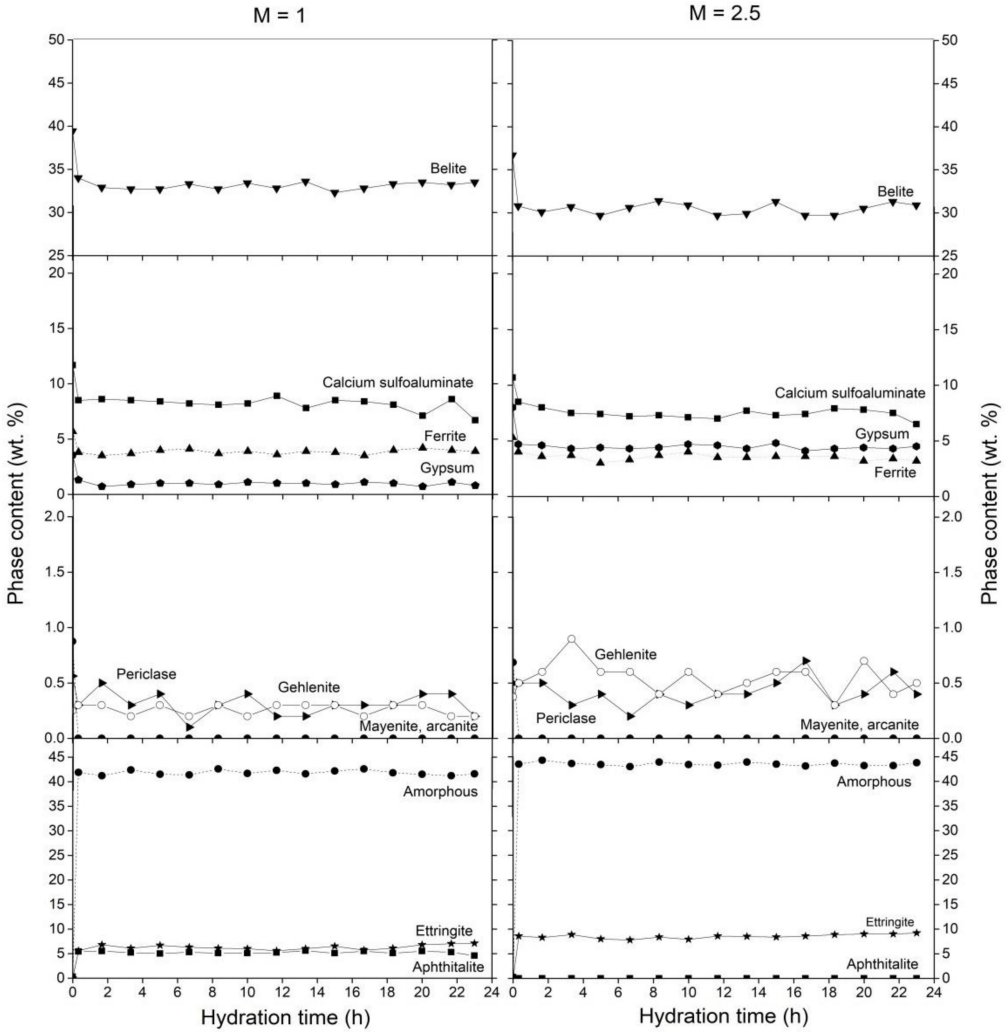

Figure 7. Phase content of clinker phases and hydrates in the cement pastes with M = 1 and M = 2.5 cured at 60 °C during first 24 h of hydration.

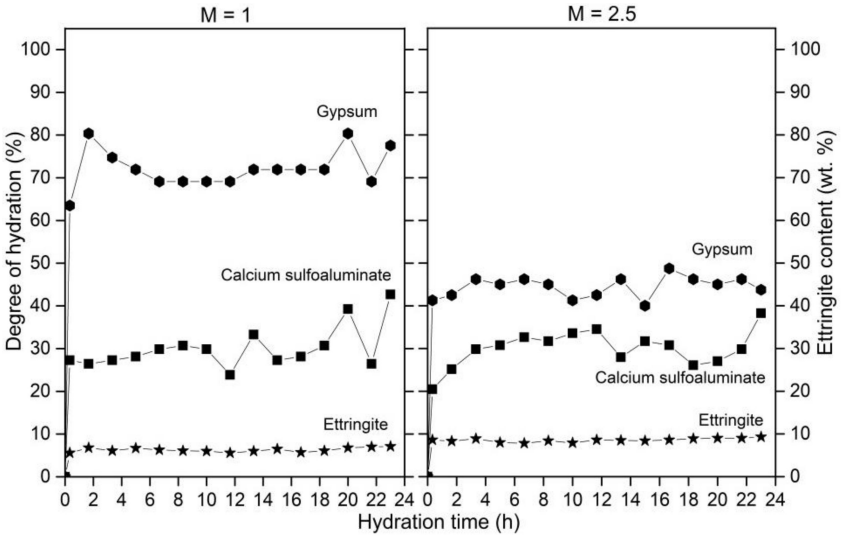

Figure 8. Degree of hydration of calcium sulfoaluminate and gypsum with ettringite content during first 24 h of hydration of the M = 1 and M = 2.5 samples at 60 °C.

At a molar ratio of 2.5, the following phases were identified: belite, calcium sulfoaluminate, ferrite, gypsum, gehlenite, periclase, and ettringite, in addition to amorphous content.

Most of the calcium sulfoaluminate and gypsum were dissolved in the first 20 min of hydration, with the calcium sulfoaluminate content reducing from 10.7 wt. % to 8.5 wt. %, and the gypsum decreasing from 8.0 wt. % to 4.7 wt. %. The degree of hydration of calcium sulfoaluminate was 38.2% at 24 h, while the degree of hydration of gypsum was 43.8% (Figure 8). 8.6 wt. % of ettringite precipitated in 20 min hours, consecutively its content did not change significantly. After 24 h, 9.2 wt. % of ettringite was measured. The clinker phases belite, ferrite, periclase, and gehlenite did not show any significant change after 20 min of hydration, while mayenite, arcanite, and aphthitalite were not detected. The amorphous content was almost constant during hydration, maintaining levels of around 43.5 wt. %.

3.4. Ettringite during Cement Hydration

Figure 9 plots the full width at half maximum (FWHM) of (100) and (110) peaks of ettringite, while Figure 10 shows the d-values of (100) and (110) peaks of ettringite, both as a function of time.

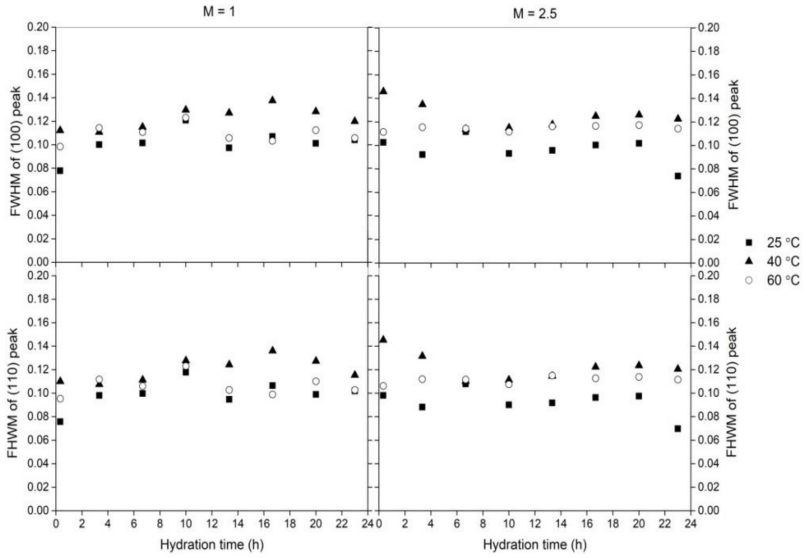

Figure 9. Full width at half maximum (FWHM) of (100) and (110) peaks of ettringite during first 24 h of hydration.

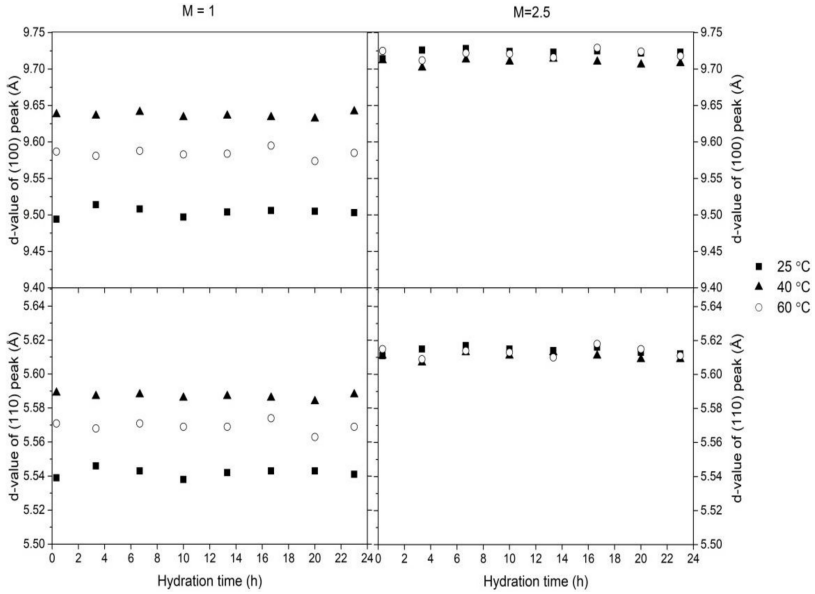

Figure 10. D-values of (100) and (110) peaks of ettringite during first 24 h of hydration.

The results of the mixture with a molar ratio of 1 at 25 °C showed that the FWHMs of (100) and (110) peaks of ettringite increased up to 10 h of hydration. After 13.3 h, however, the values decreased then remained almost constant up to 24 h of hydration. At 40 °C, the FWHM was roughly constant up to 10 h, at which point it showed a slight increase and then stayed constant up to 24 h. At 60 °C, an increase in the FWHM was observed up to 10 h of hydration, followed by a decrease. The results show that FWHMs values were the lowest at a temperature of 25 °C.

At a molar ratio of 2.5 at 25 °C, results showed that FWHMs of (100) and (110) peaks of ettringite were roughly constant until 6.6 h, after which point they increased significantly until 10 h but then started to decrease. Between 10 and 22 h of hydration the FWHM was almost constant, until 23 h, when it significantly decreased. At 40 °C FWHMs of (100) and (110) peaks of ettringite were the highest at 20 min of hydration. The values then decreased until 6.6 h, after which time the values did not significantly change up to 24 h of hydration. At 60 °C, the FWHMs of (100) and (110) peaks of ettringite were roughly constant throughout the entire hydration period. The results show that FWHMs were the lowest at 25 °C.

The d-values of (100) and (110) peaks of ettringite at a molar ratio of 1 (M = 1) were almost constant at 25 °C, with slightly lower values at 20 min of hydration. At 40 °C, the d-values of (100) and (110) peak of ettringite did not change significantly in the first 24 h of hydration. At 60 °C, the d-values of (100) and (110) peaks of ettringite remained constant up to 20 h of hydration, at which point the values decreased. D-values were lowest at ambient temperatures, and highest at 40 °C.

The results of the mixture with a molar ratio of 2.5 (M = 2.5) show that at 25, 40 and 60 °C the d-values of (100) and (110) peaks of ettringite did not change significantly with time and temperature.

4. Discussion

During the first 24 h, belite calcium sulfoaluminate cement pastes with different molar ratio of calcium sulfate to calcium sulfoaluminate mainly consisted of belite and calcium sulfoaluminate with ferrite and gypsum. At an early age the calcium sulfoaluminate reacted with gypsum and water to form ettringite, according to Equation (1).

At 25, 40 and 60 °C, the main and only detected hydrate phase formed in both cement pastes (calcium sulfate to calcium sulfoaluminate molar ratios of 1 and 2.5) was ettringite. The results show that the hydration started immediately after adding the defined amount of water to the unhydrated cement with the dissolution of calcium sulfoaluminate and gypsum and the formation of ettringite. Aluminum hydroxide, which, according to Equation (1), precipitates with ettringite, was not detected by PXRD in either mixture, which relates to its amorphous character at an early age [5,15,51]. The amorphous content in the mixtures was attributed mainly to the residual water, and to a lesser extent to noncrystalline phases [39,52], in this case aluminum hydroxide, which is formed at an earlier stage. C-S-H precipitates later, with the hydration of belite [7,18]. Amorphous content increased at ambient temperatures with hydration time for both molar ratios; however, at elevated temperatures, it remained constant during hydration. This is due to the slower formation of ettringite at an ambient temperature, and consequently aluminum hydroxide formed with it, leading to a continuous increase in amorphous content. At elevated temperatures, ettringite precipitated very fast at the beginning of the hydration and only slowly increased after, therefore the amount of amorphous content did not change significantly. Furthermore, monosulfate, which was predicted according to Equation (2), was not detected during the first 24 h of hydration, which was due to poor crystallinity or small crystalline size [15,20,30], and which would have contributed to the amorphous content measured [53]. The amount of belite did not change significantly in the first 24 h of hydration, because belite exhibits low reactivity at early ages and reacts at a later hydration time [54]. Due to its low and slow solubility, ferrite content did not decrease with hydration time [55]. Moreover, the minor phase mayenite, which is known to rapidly dissolve and increases the

aluminum and calcium ion concentration [56], accordingly was depleted within the first 20 min of hydration. Mayenite can accelerate early hydration by reacting with water and gypsum and therefore accelerate the formation of ettringite [56]. Due to their low reactivity, periclase and gehlenite are considered inert in these types of cements [57], therefore their amounts did not change during hydration. After the start of hydration, the minor clinker phase arcanite was not detected in the cement pastes, because it is a rapid soluble alkali sulfate phase [36,58] that was already depleted. Aphthitalite, however, which is also a rapid soluble phase [36], was depleted after 20 min of hydration at 25 °C. On the other hand, during hydration at 40 °C and 60 °C, it precipitated in M = 1 sample. At 40 °C it precipitated after 1.6 h, while at 60 °C it was detected already at 20 min of hydration. Moreover, a much higher amount of aphthitalite precipitated at 60 °C compared to at 40 °C, indicating that with increasing temperature above ambient, the formation of aphthitalite is increased due to a higher release of alkalis from the clinker phases. Apart from alkali sulfates present in the clinkers, the alkalis, which are incorporated in the main clinker phases, mainly in calcium sulfoaluminate [37], could be released through the dissolution of these phases [37,59] as well, reacting with sulfate from the gypsum, and form the alkali sulfate phase aphthitalite. Namely, another alkali sulfate phase thenardite (Na_2SO_4) was found forming in calcium sulfoaluminate cements at high alkalinity, explained as a product of excess alkalis initially reacting with anhydrite, which retards calcium sulfoaluminate hydration and ettringite formation [60]. This mechanism could also explain the lower amount of precipitated ettringite in samples at M = 1 in comparison to M = 2.5 at 40 and 60 °C. Furthermore, aphthitalite was detected only at a lower molar ratio of M = 1, probably due to a higher proportion of clinker and a consequently larger amount of alkalis introduced into the hydrating system in addition to lower gypsum content. Moreover, aphthitalite was present only at the two elevated temperatures, as crystallization is highly temperature-dependent [61].

At ambient temperatures, more calcium sulfoaluminate reacted in the cement pastes with a higher molar ratio of calcium sulfate to calcium sulfoaluminate, indicating that calcium sulfate accelerates the dissolution of calcium sulfoaluminate [14]. However, at elevated temperatures, less calcium sulfoaluminate was consumed in the samples with a higher molar ratio of calcium sulfate to calcium sulfoaluminate. Furthermore, at a molar ratio of M = 1, gypsum had a higher degree of reaction, meaning a higher amount of gypsum was dissolved in comparison to samples with a molar ratio of 2.5. Moreover, the results showed that, at ambient temperatures, the hydration of calcium sulfoaluminate is more rapid in a mixture with higher calcium sulfate content, which is also in accordance with data from the literature [6,55]. The rate of hydration could also influence the fact that cement with M = 2.5 had a slightly higher specific surface area in comparison cement with M = 1, which could also enhance the reactivity of cement [10]. Nevertheless, both cements have similar particle size distribution (Figure 1). In addition, at all temperatures, the amount of ettringite precipitated after 24 h was higher in the mixtures with a greater amount of calcium sulfate. It has already been reported that more ettringite is formed when the addition of gypsum is higher [9]. However, the ettringite precipitation rate at a lower molar ratio was slower at the beginning, in comparison to higher molar ratios, where the precipitation rate was very fast and more constant over the first 24 h of hydration.

Comparing the results at different temperatures, it can be seen that hydration was accelerated at elevated temperatures in comparison to ambient temperatures, for both molar ratios of calcium sulfate to calcium sulfoaluminate of 1 and 2.5. At 25 °C most of the calcium sulfoaluminate and gypsum reacted in the first 3 h of hydration, while at 40 and 60 °C these reactions occurred in the first 1.6 h and 20 min, respectively. This is in line with the previous study investigating hydration of belite-calcium sulfoaluminate cements [24], where isothermal calorimetry results showed the main exothermic peak of cement paste cured at 20 °C right after 3 h of hydration and after 75 and 30 min at 40 and 60 °C, respectively. Accelerated hydration at an elevated temperature has also been observed by other researchers, not only in calcium sulfoaluminate cements, but also in

Portland cement, calcium aluminate cements and blended cements [18,62–64]. On the other hand, the degree of hydration was much lower at elevated temperatures in comparison to ambient temperature, with less calcium sulfoaluminate and gypsum consumed and, consequently, a lower precipitation of ettringite. A decrease in the amount of ettringite at elevated temperatures was also observed by Lothenbach et al. [65], due to less time for the diffusion of dissolved ions and precipitation of hydration products [65–67]. However, the degree of reaction of calcium sulfoaluminate was comparable at 40 °C and 60 °C, and the amount of ettringite was also almost the same. Only at 25 °C in the cement paste with a molar ratio of calcium sulfate to calcium sulfoaluminate of 1 gypsum was completely depleted after 3 h of hydration.

According to Scherrer's Equation [68], which can be used for the determination of the particle sizes, the FWHM is inversely proportional to crystallite size [68], meaning the broader the peak (i.e, the higher the FWHM), the smaller the crystallite size. The FWHMs of (100) and (110) peak of ettringite at a molar ratio of calcium sulfate to calcium sulfoaluminate of 1 were lowest at 25 °C, indicating that crystallite size decreased at elevated temperatures in comparison to ambient temperature due to faster formation of ettringite at increased temperatures, which was already indicated in previous literature data by microscopical observations [24,65]. Crystallite sizes were, however, higher at 40 °C compared to 60 °C. Differences in the FWHMs between the molar ratio of calcium sulfate to calcium sulfoaluminate 1 and 2.5 were not significant, indicating crystallite sizes did not vary with a different gypsum amount.

The structure of ettringite is open and flexible, and thus allows other atoms to be incorporated into the structure [69], resulting in variable d-values. Ettringite has the capability to substitute Ca^{2+}, Al^{3+}, $SO_4{}^{2-}$ sites with other anions or cations, such as Sr^{2+}, Ba^{2+}, or Pb^{2+} for the Ca^{2+} site, Cr^{3+}, Si^{4+}, or Fe^{3+} for the Al^{3+} site, and $CO_3{}^{2-}$, Cl^{-}, or OH^{-} for the $SO_4{}^{2-}$ site and also other ions [70,71], which have different ionic radii and can cause a change in the d-spacings of the ettringite, e.g., larger ionic radii of the substitute ions increase the cell parameters [72]. The d-spacings of (100) and (110) peaks of ettringite at a molar ratio of calcium sulfate to calcium sulfoaluminate of 1 and 2.5 at each temperature during hydration only slightly changed. There was, however, a significant difference when comparing values at 25, 40 and 60 °C at a molar ratio of calcium sulfate to calcium sulfoaluminate of 1, for which the results showed that d-spacings are lowest at 25 °C, and increased at an elevated temperature. D-values were, however, higher at 40 °C compared to 60 °C. It is therefore evident that the d-spacing changes with temperature, suggesting the incorporation of ions with larger ion radii or a higher ion intake for ettringite at elevated temperatures, as more ions are released from the main clinker phases. However, at a molar ratio of calcium sulfate to calcium sulfoaluminate of 2.5 these differences in temperature were almost negligible, probably due to the lower clinker proportion at this molar ratio, and less potential substitution ions available to incorporate into the ettringite structure. On the other hand, comparing the results at different molar ratios of calcium sulfate to calcium sulfoaluminate, it is evident that the d-values of (100) and (110) peaks of ettringite were greater when the molar ratio was 2.5.

5. Conclusions

The influence of different temperatures on the phase composition of belite-calcium sulfoaluminate cement pastes with M-values of 1 and 2.5 during the first 24 h of hydration was studied at 25, 40 and 60 °C.

The amount of gypsum and calcium sulfoaluminate decreased with time at all curing temperatures, due to the formation of ettringite. More calcium sulfoaluminate and gypsum were consumed, and, consequently, the amount of ettringite was higher in the samples cured at 25 °C in comparison to those cured at elevated temperatures at both molar ratios (M = 1 and 2.5). Increasing the temperature from 40 °C to 60 °C also affects the formation of ettringite and the hydration degree of clinker phases; however not that significantly as in comparison to ambient temperature. At ambient temperatures less calcium sulfoaluminate

reacted in the samples with a lower calcium sulfate to calcium sulfoaluminate molar ratio, while at elevated temperatures the degree of hydration of calcium sulfoaluminate was higher at a lower calcium sulfate to calcium sulfoaluminate molar ratio. Moreover, at 25 °C, in the samples with a calcium sulfate to calcium sulfoaluminate molar ratio of 1, the gypsum was completely consumed by the reaction with calcium sulfoaluminate to form ettringite, while it remained present in all other mixtures.

Furthermore, hydration was accelerated at elevated temperatures in comparison to an ambient temperature, as a higher degree of hydration of calcium sulfoaluminate was observed at the beginning of the hydration, and more ettringite was formed.

Full width at half maximum of ettringite peaks increased at elevated temperatures at a molar ratio of calcium sulfate to calcium sulfoaluminate 1 and 2.5, indicating a decrease in crystallite size at elevated temperatures, due to a higher degree of hydration and faster precipitation of ettringite. However, different gypsum amounts (M-value) did not affect crystallite sizes of ettringite.

At a molar ratio of calcium sulfate to calcium sulfoaluminate 1, the d-values of ettringite peaks increased at elevated temperatures, suggesting a higher ion uptake in the ettringite structure as more ions were released from the cement clinker. At a molar ratio of 2.5, however, there is no significant difference in the d-values, due to a higher addition of gypsum, the cement mixture contains less clinker is in and consequently less substitute ions are available to incorporate into the ettringite.

Author Contributions: Conceptualization, S.D., C.L.L. and M.B.; methodology, S.D., C.L.L. and M.B.; analysis, C.L.L. and M.B.; writing—original draft preparation, M.B.; writing—review and editing, M.B., S.D., C.L.L.; funding acquisition, M.B., S.D., C.L.L. All authors have read and agreed to the published version of the manuscript.

Funding: The research is performed within the Young researcher program (contract number 1000-18-1502) and bilateral project SI-AT Effect of clinkering process on the mineralogy of belite-sulfoaluminate cement clinker (BI-AT/18-19-014), both supported by the Slovenian Research Agency and the Austrian Agency for International Cooperation in Education and Research (OeAD) from grant SI-16-2018.

Acknowledgments: The Metrology Institute of the Republic of Slovenia is acknowledged for the use of XRF.

Conflicts of Interest: The authors declare no conflict of interest.

References

1. Álvarez-Pinazo, G.; Cuesta, A.; García-Maté, M.; Santacruz, I.; Losilla, E.R.; Sanfélix, S.G.; Fauth, F.; Aranda, M.A.G.; De la Torre, A.G. In-Situ Early-Age Hydration Study of Sulfobelite Cements by Synchrotron Powder Diffraction. *Cem. Concr. Res.* **2014**, *56*, 12–19. [CrossRef]
2. Senff, L.; Castela, A.; Hajjaji, W.; Hotza, D.; Labrincha, J.A. Formulations of Sulfobelite Cement through Design of Experiments. *Constr. Build. Mater.* **2011**, *25*, 3410–3416. [CrossRef]
3. Álvarez-Pinazo, G.; Santacruz, I.; León-Reina, L.; Aranda, M.A.G.; De la Torre, A.G. Hydration Reactions and Mechanical Strength Developments of Iron-Rich Sulfobelite Eco-Cements. *Ind. Eng. Chem. Res.* **2013**, *52*, 16606–16614. [CrossRef]
4. Álvarez-Pinazo, G.; Santacruz, I.; Aranda, M.A.G.; De la Torre, Á.G. Hydration of Belite–Ye'elimite–Ferrite Cements with Different Calcium Sulfate Sources. *Adv. Cem. Res.* **2016**, *28*, 529–543. [CrossRef]
5. Bullerjahn, F.; Zajac, M.; Skocek, J.; Ben Haha, M. The Role of Boron during the Early Hydration of Belite Ye'elimite Ferrite Cements. *Constr. Build. Mater.* **2019**, *215*, 252–263. [CrossRef]
6. Morin, V.; Termkhajornkit, P.; Huet, B.; Pham, G. Impact of Quantity of Anhydrite, Water to Binder Ratio, Fineness on Kinetics and Phase Assemblage of Belite-Ye'elimite-Ferrite Cement. *Cem. Concr. Res.* **2017**, *99*, 8–17. [CrossRef]
7. Bullerjahn, F.; Schmitt, D.; Ben Haha, M. Effect of Raw Mix Design and of Clinkering Process on the Formation and Mineralogical Composition of (Ternesite) Belite Calcium Sulphoaluminate Ferrite Clinker. *Cem. Concr. Res.* **2014**, *59*, 87–95. [CrossRef]
8. Cuberos, A.J.M.; De la Torre, Á.G.; Álvarez-Pinazo, G.; Martín-Sedeño, M.C.; Schollbach, K.; Pöllmann, H.; Aranda, M.A.G. Active Iron-Rich Belite Sulfoaluminate Cements: Clinkering and Hydration. *Environ. Sci. Technol.* **2010**, *44*, 6855–6862. [CrossRef]
9. Jeong, Y.; Hargis, C.W.; Chun, S.-C.; Moon, J. The Effect of Water and Gypsum Content on Strätlingite Formation in Calcium Sulfoaluminate-Belite Cement Pastes. *Constr. Build. Mater.* **2018**, *166*, 712–722. [CrossRef]
10. Rossetto, C.M.; Ichikawa, R.U.; Martinez, L.G.; Carezzato, G.L.; Carvalho, A.M.G.; Turrillas, X. In Situ Hydration of Sulfoaluminate Cement Mixtures Monitored by Synchrotron X-Ray Diffraction. *MSF* **2018**, *930*, 153–157. [CrossRef]

11. Liao, Y.; Wei, X.; Li, G. Early Hydration of Calcium Sulfoaluminate Cement through Electrical Resistivity Measurement and Microstructure Investigations. *Constr. Build. Mater.* **2011**, *25*, 1572–1579. [CrossRef]
12. Martín-Sedeño, M.C.; Cuberos, A.J.M.; De la Torre, Á.G.; Álvarez-Pinazo, G.; Ordónez, L.M.; Gateshki, M.; Aranda, M.A.G. Aluminum-Rich Belite Sulfoaluminate Cements: Clinkering and Early Age Hydration. *Cem. Concr. Res.* **2010**, *40*, 359–369. [CrossRef]
13. Morin, V.; Walenta, G.; Gartner, E.; Termkhajornkit, P.; Baco, I.; Casabonne, J.M. Hydration of a Belite-Calcium Sulfoaluminate-Ferrite cement: Aether^{TM}. In Proceedings of the 13th International Congress on the Chemistry of Cement, Madrid, Spain, 3–8 July 2011.
14. Winnefeld, F.; Martin, L.H.J.; Müller, C.J.; Lothenbach, B. Using Gypsum to Control Hydration Kinetics of CSA Cements. *Constr. Build. Mater.* **2017**, *155*, 154–163. [CrossRef]
15. Winnefeld, F.; Barlag, S. Calorimetric and Thermogravimetric Study on the Influence of Calcium Sulfate on the Hydration of Ye'elimite. *J. Therm. Anal. Calorim.* **2010**, *101*, 949–957. [CrossRef]
16. Glasser, F.P.; Zhang, L. High-Performance Cement Matrices Based on Calcium Sulfoaluminate–Belite Compositions. *Cem. Concr. Res.* **2001**, *31*, 1881–1886. [CrossRef]
17. Sahu, S.; Havlica, J.; Tomkova, V.; Majling, J. Hydration Behaviour of Sulphoaluminate Belite Cement in the Presence of Various Calcium Sulphates. *Thermochim. Acta* **1991**, *175*, 45–52. [CrossRef]
18. Zhang, L.; Glasser, F.P. Hydration of Calcium Sulfoaluminate Cement at Less than 24 h. *Adv. Cem. Res.* **2002**, *14*, 15. [CrossRef]
19. García-Maté, M.; De la Torre, A.G.; León-Reina, L.; Losilla, E.R.; Aranda, M.A.G.; Santacruz, I. Effect of Calcium Sulfate Source on the Hydration of Calcium Sulfoaluminate Eco-Cement. *Cem. Concr. Compos.* **2015**, *55*, 53–61. [CrossRef]
20. Zajac, M.; Skocek, J.; Bullerjahn, F.; Ben Haha, M. Effect of Retarders on the Early Hydration of Calcium-Sulpho-Aluminate (CSA) Type Cements. *Cem. Concr. Res.* **2016**, *84*, 62–75. [CrossRef]
21. Beltagui, H.; Jen, G.; Whittaker, M.; Imbabi, M.S. The Influence of Variable Gypsum and Water Content on the Strength and Hydration of a Belite-Calcium Sulphoaluminate Cement. *Adv. Appl. Ceram.* **2017**, *116*, 199–206. [CrossRef]
22. Chen, I.A.; Juenger, M.C.G. Synthesis and Hydration of Calcium Sulfoaluminate-Belite Cements with Varied Phase Compositions. *J. Mater. Sci.* **2011**, *46*, 2568–2577. [CrossRef]
23. Kaufmann, J.; Winnefeld, F.; Lothenbach, B. Stability of Ettringite in CSA Cement at Elevated Temperatures. *Adv. Cem. Res.* **2016**, *28*, 251–261. [CrossRef]
24. Borštnar, M.; Daneu, N.; Dolenec, S. Phase Development and Hydration Kinetics of Belite-Calcium Sulfoaluminate Cements at Different Curing Temperatures. *Ceram. Int.* **2020**, *46*, 29421–29428. [CrossRef]
25. Jakob, C.; Jansen, D.; Ukrainczyk, N.; Koenders, E.; Pott, U.; Stephan, D.; Neubauer, J. Relating Ettringite Formation and Rheological Changes during the Initial Cement Hydration: A Comparative Study Applying XRD Analysis, Rheological Measurements and Modeling. *Materials* **2019**, *12*, 2957. [CrossRef] [PubMed]
26. Hesse, C.; Goetz-Neunhoeffer, F.; Neubauer, J.; Braeu, M.; Gaeberlein, P. Quantitative in Situ X-Ray Diffraction Analysis of Early Hydration of Portland Cement at Defined Temperatures. *Powder Diffr.* **2009**, *24*, 112–115. [CrossRef]
27. Jansen, D.; Spies, A.; Neubauer, J.; Ectors, D.; Goetz-Neunhoeffer, F. Studies on the Early Hydration of Two Modifications of Ye'elimite with Gypsum. *Cem. Concr. Res.* **2017**, *91*, 106–116. [CrossRef]
28. Zajac, M.; Skocek, J.; Bullerjahn, F.; Lothenbach, B.; Scrivener, K.; Ben Haha, M. Early Hydration of Ye'elimite: Insights from Thermodynamic Modelling. *Cem. Concr. Res.* **2019**, *120*, 152–163. [CrossRef]
29. Merlini, M.; Artioli, G.; Meneghini, C.; Cerulli, T.; Bravo, A.; Cella, F. The Early Hydration and the Set of Portland Cements: In Situ X-Ray Powder Diffraction Studies. *Powder Diffr.* **2007**, *22*, 201–208. [CrossRef]
30. Gastaldi, D.; Paul, G.; Marchese, L.; Irico, S.; Boccaleri, E.; Mutke, S.; Buzzi, L.; Canonico, F. Hydration Products in Sulfoaluminate Cements: Evaluation of Amorphous Phases by XRD/Solid-State NMR. *Cem. Concr. Res.* **2016**, *90*, 162–173. [CrossRef]
31. Jeong, Y.; Hargis, C.W.; Kang, H.; Chun, S.-C.; Moon, J. The Effect of Elevated Curing Temperatures on High Ye'elimite Calcium Sulfoaluminate Cement Mortars. *Materials* **2019**, *12*, 1072. [CrossRef]
32. Valentini, L.; Dalconi, M.C.; Favero, M.; Artioli, G.; Ferrari, G. In-Situ XRD Measurement and Quantitative Analysis of Hydrating Cement: Implications for Sulfate Incorporation in C-S-H. *J. Am. Ceram. Soc.* **2015**, *98*, 1259–1264. [CrossRef]
33. Hesse, C.; Goetz-Neunhoeffer, F.; Neubauer, J. A New Approach in Quantitative In-Situ XRD of Cement Pastes: Correlation of Heat Flow Curves with Early Hydration Reactions. *Cem. Concr. Res.* **2011**, *41*, 123–128. [CrossRef]
34. Rietveld, H.M. A Profile Refinement Method for Nuclear and Magnetic Structures. *J. Appl. Crystallogr.* **1969**, *2*, 65–71. [CrossRef]
35. Žibret, L.; Ipavec, A.; Kramar, S. Microstructure of Belite Sulfoaluminate Clinker and Its Influence on Clinker Reactivity. In Proceedings of the International Workshop on Calcium Sulfoaluminate Cements, Murten, Switzerland, 4 June 2018; Volume 2018, p. 1.
36. Taylor, H.F.W. *Cement Chemistry*, 2nd ed.; T. Telford: London, UK, 1997; ISBN 978-0-7277-2592-9.
37. Dolenec, S.; Šter, K.; Borštnar, M.; Nagode, K.; Ipavec, A.; Žibret, L. Effect of the Cooling Regime on the Mineralogy and Reactivity of Belite-Sulfoaluminate Clinkers. *Minerals* **2020**, *10*, 910. [CrossRef]
38. NSAI. *EN 196-6:2018. Methods of Testing Cement-Part 6: Determination of Fineness*; NSAI: Dublin, Ireland, 2010.
39. Snellings, R. X-ray powder diffraction applied to cement. In *A Practical Guide to Microstructural Analysis of Cementitious Materials*; CRC Press: Boca Raton, FL, USA, 2016; pp. 126–195.
40. Cuesta, A.; De la Torre, A.G.; Losilla, E.R.; Peterson, V.K.; Rejmak, P.; Ayuela, A.; Frontera, C.; Aranda, M.A.G. Structure, Atomistic Simulations, and Phase Transition of Stoichiometric Yeelimite. *Chem. Mater.* **2013**, *25*, 1680–1687. [CrossRef]

41. Cuesta, A.; De la Torre, Á.G.; Losilla, E.R.; Santacruz, I.; Aranda, M.A.G. Pseudocubic Crystal Structure and Phase Transition in Doped Ye'elimite. *Cryst. Growth Des.* **2014**, *14*, 5158–5163. [CrossRef]
42. Mumme, W.G.; Hill, R.J.; Bushnell-Wye, G.; Segnit, E.R. Rietveld Crystal Structure Refinements, Crystal Chemistry and Calculated Powder Diffraction Data for the Polymorphs of Dicalcium Silicate and Related Phases. *Miner. Geochem.* **1995**, *1*, 35–68.
43. Redhammer, G.J.; Tippelt, G.; Roth, G.; Amthauer, G. Structural Variations in the Brownmillerite Series $Ca_2(Fe_{2-x}Al_x)O_5$: Single-Crystal X-Ray Diffraction at 25 °C and High-Temperature X-Ray Powder Diffraction (25 °C ≤ T ≤ 1000 °C). *Am. Mineral.* **2004**, *89*, 405–420. [CrossRef]
44. Boeyens, J.; Ichharam, V. Redetermination of the Crystal Structure of Calcium Sulphate Dihydrate, $CaSO_4 \cdot 2H_2O$. Zeitschrift für Kristallographie. *New Cryst. Struct.* **2002**, *217*, 9–10.
45. Sasaki, S.; Fujino, K.; Takéuchi, Y. X-Ray Determination of Electron-Density Distributions in Oxides, MgO, MnO, CoO, and NiO, and Atomic Scattering Factors of Their Constituent Atoms. *Proc. Jpn. Acad. Ser. B* **1979**, *55*, 43–48. [CrossRef]
46. Sakakura, T.; Tanaka, K.; Takenaka, Y.; Matsuishi, S.; Hosono, H.; Kishimoto, S. Determination of the Local Structure of a Cage with an Oxygen Ion in $Ca_{12}Al_{14}O_{33}$. *Acta Cryst.* **2011**, *67*, 193–204. [CrossRef] [PubMed]
47. Gemmi, M.; Merlini, M.; Cruciani, G.; Artioli, G. Non-Ideality and Defectivity of the Akermanite-Gehlenite Solid Solution: An X-Ray Diffraction and TEM Study. *Am. Mineral.* **2007**, *92*, 1685–1694. [CrossRef]
48. Ojima, K.; Nishihata, Y.; Sawada, A. Structure of Potassium Sulfate at Temperatures from 296 K down to 15 K. *Acta Cryst. B* **1995**, *51*, 287–293. [CrossRef]
49. Okada, K.; Ossaka, J. Structures of Potassium Sodium Sulphate and Tripotassium Sodium Disulphate. *Acta Cryst. B* **1980**, *36*, 919–921. [CrossRef]
50. Goetz-Neunhoeffer, F.; Neubauer, J. Refined Ettringite ($Ca_6Al_2(SO_4)_3(OH)_{12} \cdot 26H_2O$) Structure for Quantitative X-Ray Diffraction Analysis. *Powder Diffr.* **2006**, *21*, 4–11. [CrossRef]
51. Champenois, J.-B.; Dhoury, M.; Cau Dit Coumes, C.; Mercier, C.; Revel, B.; Le Bescop, P.; Damidot, D. Influence of Sodium Borate on the Early Age Hydration of Calcium Sulfoaluminate Cement. *Cem. Concr. Res.* **2015**, *70*, 83–93. [CrossRef]
52. Cuesta, A.; Zea-Garcia, J.D.; Londono-Zuluaga, D.; De la Torre, A.G.; Santacruz, I.; Vallcorba, O.; Dapiaggi, M.; Sanfélix, S.G.; Aranda, M.A.G. Multiscale Understanding of Tricalcium Silicate Hydration Reactions. *Sci. Rep.* **2018**, *8*, 8544. [CrossRef]
53. Scrivener, K.L.; Füllmann, T.; Gallucci, E.; Walenta, G.; Bermejo, E. Quantitative Study of Portland Cement Hydration by X-Ray Diffraction/Rietveld Analysis and Independent Methods. *Cem. Concr. Res.* **2004**, *34*, 1541–1547. [CrossRef]
54. Cuberos, A.J.M.; De la Torre, Á.G.; Martín-Sedeño, M.C.; Moreno-Real, L.; Merlini, M.; Ordónez, L.M.; Aranda, M.A.G. Phase Development in Conventional and Active Belite Cement Pastes by Rietveld Analysis and Chemical Constraints. *Cem. Concr. Res.* **2009**, *39*, 833–842. [CrossRef]
55. Zajac, M.; Skocek, J.; Stabler, C.; Bullerjahn, F.; Ben Haha, M. Hydration and Performance Evolution of Belite-Ye'elimite-Ferrite Cement. *Adv. Cem. Res.* **2019**, *31*, 124–137. [CrossRef]
56. Bullerjahn, F.; Zajac, M.; Ben Haha, M.; Scrivener, K.L. Factors Influencing the Hydration Kinetics of Ye'elimite; Effect of Mayenite. *Cem. Concr. Res.* **2019**, *116*, 113–119. [CrossRef]
57. Jeong, Y.; Hargis, C.; Chun, S.; Moon, J. Effect of Calcium Carbonate Fineness on Calcium Sulfoaluminate-Belite Cement. *Materials* **2017**, *10*, 900. [CrossRef] [PubMed]
58. Halaweh, M. Effect of Alkalis and Sulfates on Portland Cement Systems. Ph.D. Thesis, University of South Florida, Tampa, FL, USA, 2006.
59. Ye, H.; Radli, A. Effect of Alkalis on Cementitious Materials: Understanding the Relationship between Composition, Structure, and Volume Change Mechanism. *J. Adv. Concr. Technol.* **2017**, *15*, 14. [CrossRef]
60. Tambara, L.U.D.; Cheriaf, M.; Rocha, J.C.; Palomo, A.; Fernández-Jiménez, A. Effect of Alkalis Content on Calcium Sulfoaluminate (CSA) Cement Hydration. *Cem. Concr. Res.* **2020**, *128*, 105953. [CrossRef]
61. López-Acevedo, V.; Viedma, C.; Gonzalez, V.; La Iglesia, A. Salt Crystallization in Porous Construction Materials. II. Mass Transport and Crystallization Processes. *J. Cryst. Growth* **1997**, *182*, 103–110. [CrossRef]
62. Escalante-Garcia, J.I.; Sharp, J.H. The Effect of Temperature on the Early Hydration of Portland Cement and Blended Cements. *Adv. Cem. Res.* **2000**, *12*, 121–130. [CrossRef]
63. Richardson, I.G.; Wilding, C.R.; Dickson, M.J. The Hydration of Blastfurnace Slag Cements. *Adv. Cem. Res.* **1989**, *2*, 147–157. [CrossRef]
64. Goergens, J.; Manninger, T.; Goetz-Neunhoeffer, F. In-Situ XRD Study of the Temperature-Dependent Early Hydration of Calcium Aluminate Cement in a Mix with Calcite. *Cem. Concr. Res.* **2020**, *136*, 106160. [CrossRef]
65. Lothenbach, B.; Winnefeld, F.; Alder, C.; Wieland, E.; Lunk, P. Effect of Temperature on the Pore Solution, Microstructure and Hydration Products of Portland Cement Pastes. *Cem. Concr. Res.* **2007**, *37*, 483–491. [CrossRef]
66. Kjellsen, K.O.; Detwiler, R.J.; Gjørv, O.E. Development of Microstructures in Plain Cement Pastes Hydrated at Different Temperatures. *Cem. Concr. Res.* **1991**, *21*, 179–189. [CrossRef]
67. Kjellsen, K.O.; Detwiler, R.J.; Gjørv, O.E. Backscattered Electron Imaging of Cement Pastes Hydrated at Different Temperatures. *Cem. Concr. Res.* **1990**, *20*, 308–311. [CrossRef]
68. Thomas, S.; Thomas, R.; Zachariah, A. *Microscopy Methods in Nanomaterials Characterization*; Elsevier: Amsterdam, The Netherlands, 2017.

69. Clark, S.M.; Colas, B.; Kunz, M.; Speziale, S.; Monteiro, P.J.M. Effect of Pressure on the Crystal Structure of Ettringite. *Cem. Concr. Res.* **2008**, *38*, 19–26. [CrossRef]
70. Chen, Q.Y.; Tyrer, M.; Hills, C.D.; Yang, X.M.; Carey, P. Immobilisation of Heavy Metal in Cement-Based Solidification/Stabilisation: A Review. *Waste Manag.* **2009**, *29*, 390–403. [CrossRef] [PubMed]
71. Chen, B.; Kuznik, F.; Horgnies, M.; Johannes, K.; Morin, V.; Gengembre, E. Physicochemical Properties of Ettringite/Meta-Ettringite for Thermal Energy Storage: Review. *Sol. Energy Mater. Sol. Cells* **2019**, *193*, 320–334. [CrossRef]
72. Suyolcu, Y.E.; Wang, Y.; Baiutti, F.; Al-Temimy, A.; Gregori, G.; Cristiani, G.; Sigle, W.; Maier, J.; van Aken, P.A.; Logvenov, G. Dopant Size Effects on Novel Functionalities: High-Temperature Interfacial Superconductivity. *Sci. Rep.* **2017**, *7*. [CrossRef]